JOURNAL OF VIROLOGY, July 2001, p. 6348–6358 Vol. 75, No. 14
0022-538X/01/$04.00+0 DOI: 10.1128/JVI.75.14.6348–6358.2001

Evidence for Retroviral Intramolecular Recombinations

JIAYOU ZHANG* AND YAN MA

Department of Microbiology and Immunology and Markey Cancer Center, University of Kentucky, Lexington, Kentucky 40536-0096

Received 1 March 2000/Accepted 14 April 2001

As a consequence of being diploid, retroviruses have a high recombination rate. Naturally occurring retroviruses contain two repeat sequences (R regions) flanking either end of their RNA genomes, and recombination between these two R regions occurs at a high rate. We deduced that recombination may occur between two sequences within the same RNA molecule (intramolecular) as well as between sequences present within two separate RNA molecules (intermolecular). Intramolecular recombination would usually result in a deletion within the progeny provirus. In this report, we demonstrate that intramolecular recombination between two identical sequences occurred within a chimeric RNA vector. In addition, high rates of recombination between two identical sequences within the same RNA molecule resulted mostly from intramolecular recombination.

The presence of two identical genomic RNA molecules in retroviral virions results in a high rate of recombination (3). The homologous intermolecular recombination rate is 4×10^{-5} per base per replication cycle (6). When nonhomologous RNA is present in these dimer RNA molecules, nonhomologous intermolecular recombination can occur, although the rate is very low, only 0.1% of the rate of essentially homologous recombination (21). A similar high rate of recombination between short region of identities in the midst of otherwise nonidentical sequences also occurs. This recombination depends on the length of sequence identity (23). Retroviruses contain two identical repeat sequences called R regions, and recombination between these two R regions has been observed (8, 10, 14).

Little is known about the physical relationship of the two RNA molecules contained in the retroviral virion. During reverse transcription, if recombination does not occur, the minus- and plus-strand DNA primers are provided almost completely intramolecularly (7). This implies that the two RNA molecules are not randomly intertwined in a virion (7). To study recombination, two different proviruses were introduced into one retroviral helper cell line. The recombinants were then judged by the expression of markers from both parental proviruses. Evidence shows that intermolecular recombinations occur frequently (6, 22). To further study recombinations between two identical sequences within the same RNA molecules, a Moloney murine leukemia virus (MLV)-based vector was constructed (19). This vector contains a complete hygromycin resistance gene (*hyg*) and a color marker reporter gene, *gfp* (green fluorescence protein). Additionally, this vector carries an extra 3′ *hyg* gene segment 290 bp in length inserted into the 3′ untranslated region of *gfp* (Fig. 1A). After one round of replication, deletion of *gfp* resulted from recombination between the downstream 3′ *hyg* sequence and the upstream 3′ *hyg* sequence. The ratio of the number of colonies without the *gfp* gene phenotype to the total number of hygromycin-resistant (Hyg^r) colonies represented the rate of recombination between the two identical sequences within the same RNA molecule. The rate of deletion in the progeny proviruses was about 62% (19). However, the high rate of recombination can be either intra- or intermolecular.

It was deduced that recombination may occur between two sequences within the same RNA molecule (intramolecular) as well as between sequences present within two separate RNA molecules (intermolecular) (17). Intramolecular recombination would result in a deletion within the progeny provirus. However, there is no direct evidence indicating that intramolecular recombination occurs. This is because, in the experiments described above, retroviral particles were able to package either two different RNA molecules or two identical RNA molecules. The deletion can result from an intramolecular event or from the recombination between a downstream sequence of one RNA molecule and the upstream sequence of the other RNA molecule. Since current technology cannot separate the viral particles containing two identical molecules (homogeneous) from those containing two different molecules (heterogeneous), deletion recombinants cannot be excluded as arising from intermolecular recombination.

In this report, we demonstrate that intramolecular recombinations actually occurred between two identical sequences within a chimeric RNA vector. Furthermore, the rate of intramolecular recombination was determined. The high rate of recombination between two identical sequences within the same RNA molecules resulted from intramolecular recombination. This observation was consistent with those regarding intramolecular transfers of DNA primers during retroviral reverse transcription (7).

MATERIALS AND METHODS

Nomenclature. Plasmids are designated as, for example, pJZ446; viruses made from these plasmids are designated as, for example, JZ446. Some infectious MLV vectors contained a 290-bp sequence derived from the 3′ end of *hyg* (Fig. 2). When the 290-bp sequence was inserted at the 5′ end of the neomycin resistance gene (*neo*) the number of nucleotides inserted is on the left of the "N" (N stands for *neo*) (for example, pL290N) (Fig. 2C). When the 290-bp sequence was inserted at the 3′ end of *neo*, the number of nucleotides inserted is on the right of the "N" (for example, pLN290) (Fig. 2B). An infectious MLV-based vector contained an 80-bp sequence derived from the 5′ end of the herpes

* Corresponding author. Mailing address: Combs Research Bldg., Room 206, University of Kentucky, 800 Rose St., Lexington, KY 40536-0096. Phone: (859) 257-4456. Fax: (859) 257-8940. E-mail: jzhan1@pop.uky.edu.

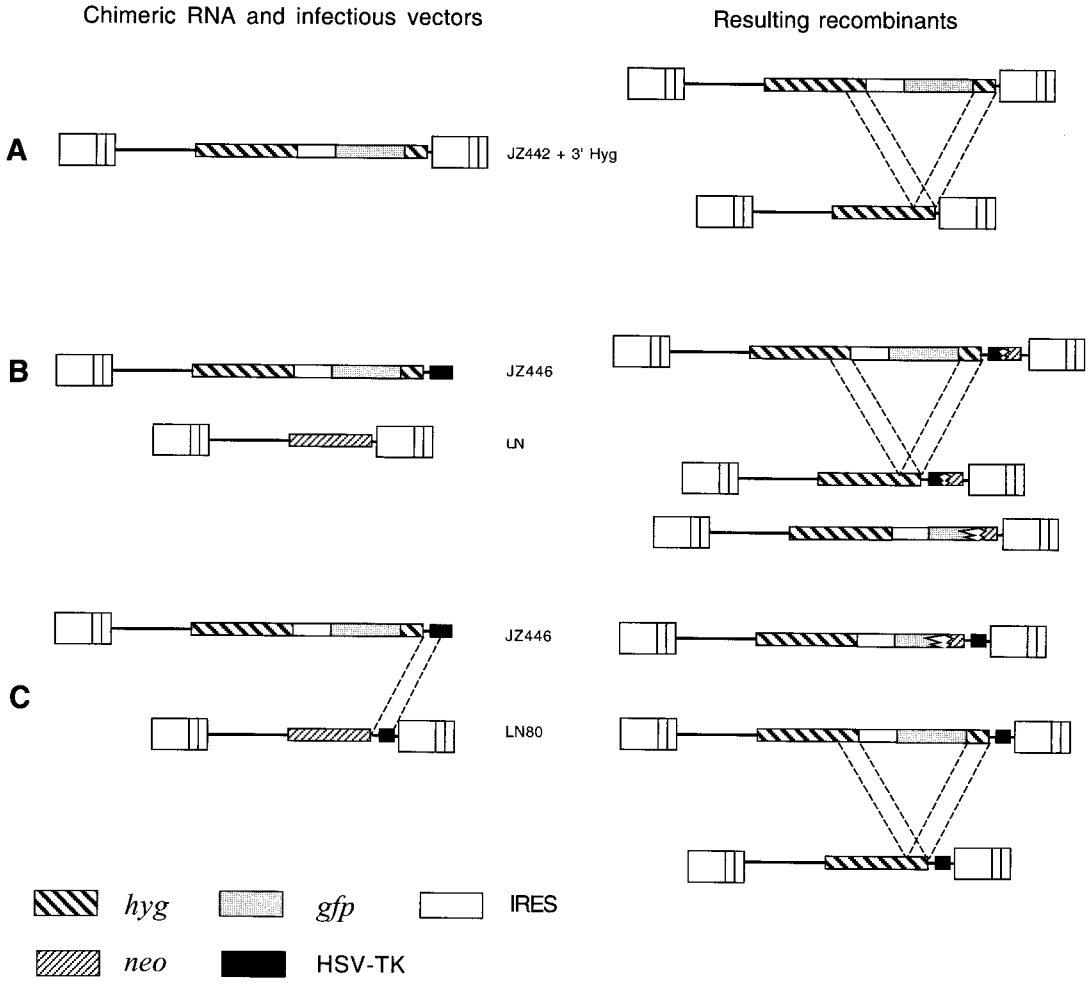

FIG. 1. Structures of retrovirus vectors used to determine the recombination rate between two identical sequences in the same RNA molecule. (A) Structure of a retrovirus containing two identical sequences. JZ422 + 3′ Hyg contains *hyg, gfp*, and an additional 290 bp of the 3′ *hyg* sequence downstream of *gfp*. After one round of replication, the downstream 3′ *hyg* sequence will recombine with the identical upstream *hyg* sequence and result in the deletion of *gfp*. Recombinants, therefore, contain only *hyg*. Dotted lines between the two recombinants indicate the identical 3′ *hyg* sequences, (B) Structures of a chimeric RNA, infectious virus vectors, and resulting recombinants. JZ446 contains only the 5′ MLV LTR, while the infectious vector LN contains two MLV LTRs. JZ446 contains *hyg, gfp*, and an additional 290 bp of the 3′ *hyg* sequence downstream of *gfp*. Recombinant proviruses, which contain *hyg*, form only when recombination occurs between the JZ446 and the infectious vector so that *hyg* is flanked by two LTRs. Recombinations between JZ446 and LN are nonhomologous (22). Most recombinations between JZ446 and LN destroy *gfp*. (C) Structures of a chimeric RNA and infectious virus vector containing 80-bp sequence identities and resulting recombinants. LN80 is identical to LN except for containing an 80-bp sequence in common with JZ446. After one round of replication, most recombinants utilized the 80-bp sequence identities to recombine with JZ446 to form a recombinant containing *gfp* flanked by two identical 290-bp sequences within the same RNA molecule. Eighty-three percent of recombinants with the two identical 290-bp sequences have undergone an intramolecular recombination resulting in a deletion of *gfp*. The dotted lines between JZ446 and LN80 indicate the identical 80-bp sequences; the dotted lines between the two recombinants indicate the identical 290-bp sequences.

simplex virus (HSV) thymidine kinase (TK) poly (A) addition signal from the chimeric RNA vector JZ446. Since the 80-bp sequence was inserted at the 3′ end of *neo*, the number of nucleotides inserted is on the right of the "N," and the vector was designated pLN80.

Vector constructions. All recombinant techniques were carried out according to conventional procedures (15). All vector sequences are available upon request.

(i) Construction of pJZ211 and pJZ446. pJZ211 (Fig. 2), the spleen necrosis virus (SNV) vector, and the truncated MLV vector containing only *hyg* were previously described (22). The chimeric RNA vector pJZ446 (Fig. 3), derived also from SNV, contained a deletion in the U3 region of its 3′ SNV long terminal repeat (LTR) and an *Xho*I restriction site linker in the deletion site (Fig. 4). The vector also contains a truncated MLV vector between the two SNV LTRs, in the opposite transcriptional orientation to the SNV LTRs. This truncated MLV vector carried *hyg*, *gfp*, and an IRES (internal ribosome entry segment) sequence between the two genes. An HSV TK poly (A) addition signal replaced the deleted 3′ MLV LTR. The IRES sequence of encephalomyocarditis virus origin allows the ribosome to bind to the internal AUG and initiate translation of *gfp* independently of *hyg* (1, 2). pJZ442 + 3′ Hyg (Fig. 1A) (19) is an MLV vector containing *hyg* and *gfp* separated by an IRES sequence plus an additional 3′ *hyg* segment at the 3′ *gfp* gene. The *Sgf*I-*Hin*dIII (2.4-kb) fragment isolated from pJZ442 + 3′ Hyg, containing the 3′ end of *hyg*, the IRES sequence, *gfp*, and an additional copy of the 3′ *hyg* sequence, was inserted into the *Sgf*I and *Hin*dIII sites of pJZ211. The resulting plasmid was designated pJZ446.

(ii) Construction of pLN, pLN290, pL290N, pL290N290, and pLN80. All infectious vectors in this study are *neo*-carrying MLV-based vectors. Vector pLN (13) contains *neo* flanked by two LTRs (Fig. 1B). pLN290, pL290N, and pL290N290 (Fig. 2B to D and 3B to D) contain one or two copies of the 3′ end of *hyg* and were described previously (19, 23). In pLN80, an 80-bp sequence derived from the 5′ end of the HSV TK poly(A) addition signal was inserted into

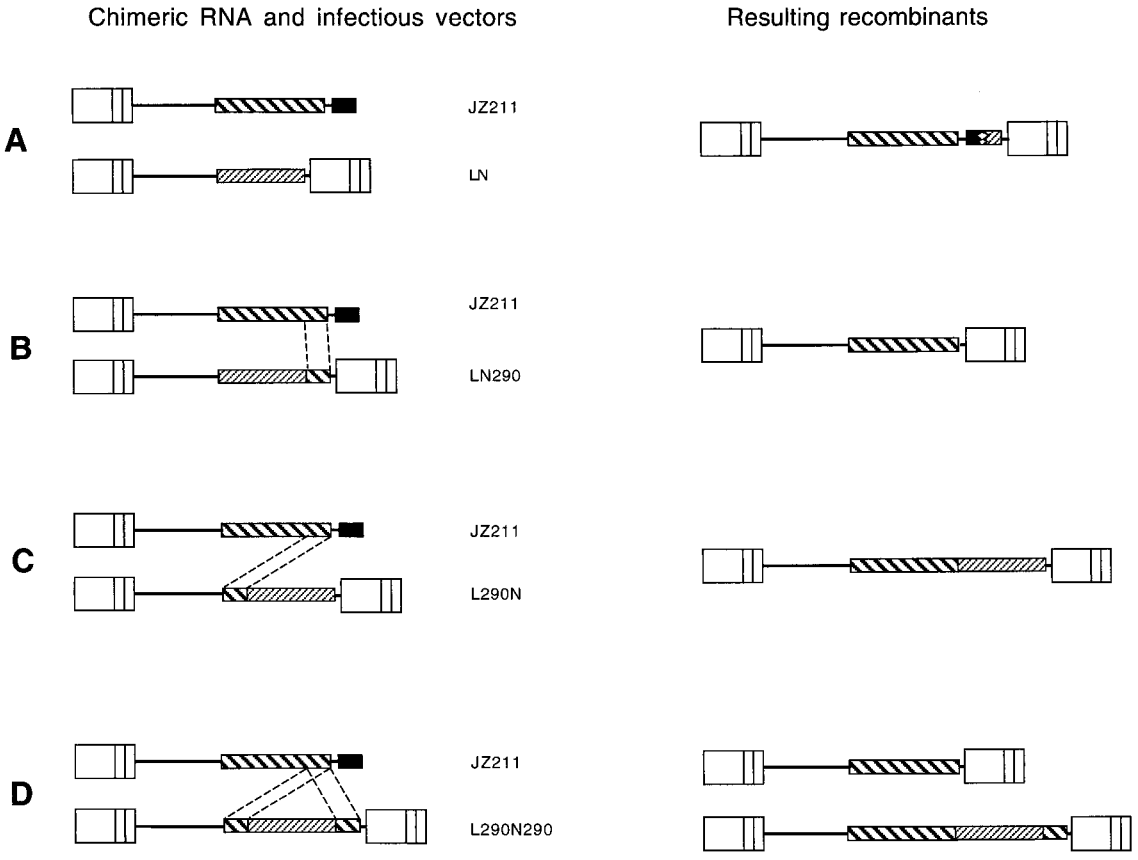

FIG. 2. Chimeric RNA vector JZ211, infectious virus vectors, and resulting recombinants. JZ211 contains only the 5′ MLV LTR, while the infectious vectors LN, LN290, LN290N, and L290N290 contain two MLV LTRs. The recombinant proviruses containing *hyg* form only when recombination occurs between JZ211 and the infectious vector such that *hyg* is flanked by two LTRs. Recombinations between JZ211 and LN are nonhomologous (22). Most recombinations between JZ211 and LN290, LN290N, and L290N290 occurred between the identical 290-bp sequences. The dotted lines between the chimeric RNA vector and the infectious vectors indicate the identical 290-bp 3′ *hyg* sequences.

the 3′ untranslated region of *neo* (Fig. 1C). Therefore, pLN80 was identical to pLN except for containing the additional 80-bp sequence. To insert the 80-bp sequence of the TK segment into pLN, the TK sequence within JZ446 was amplified by PCR. The first primer hybridized with the MLV packaging signal, and the second primer (5′-TCTTATCGATTGCCGTCATAGCGC-3′) hybridized with the 3′ end of the TK segment. The *Hin*dIII-*Cla*I fragment of the amplified DNA was inserted between the *Hin*dIII and *Cla*I sites of pLNCX (13). The inserted sequence in the resulting vector was confirmed by DNA sequencing.

(iii) Construction of JZ525 and YM2. The pJZ525 construct (Fig. 5A), from 5′ to 3′, was assembled as follows. The 2.5-kb *Bam*HI-*Not*I fragment (from positions 1630 to 4112) was isolated from pJZ442 + 3′ Hyg (Fig. 1A) (19) and contained *hyg*, the IRES, and *gfp*. The 0.6-kb *Not*I-*Nde*I fragment (positions 4113 to 4650) contained an identical IRES sequence. The 5.4-kp *Nde*I-*Bam*HI fragment (positions 4651 to 1629) was isolated from pLN (13) and contained *neo* and the two MLV LTRs. The *Nco*I site within *neo* was digested, followed by repair with the Klenow fragment. *Nco*I digestion created two DNA ends that contained a four-base overhang. Repair of the overhang by the Klenow fragment created two blunt ends. Ligation of these two blunt ends with T4 ligase created a 4-bp insertion, which shifted the *neo* open reading fragment by one (+1). The retroviral vector YM2 was identical to JZ425 except that YM2 contained a different frameshift mutation at the *Sgf*I site within the *hyg* open reading frame, while *neo* was functional.

Introduction of a single chimeric RNA vector and a single infectious vector into helper cell line PG13. Retroviral vectors and protocols used to measure rates of recombination have been described previously (22). To study recombination between chimeric and infectious MLV RNAs, a chimeric RNA vector DNA (pJZ446 or pJZ211) was transfected into the SNV C3A2 helper cell line (containing the SNV *gag-pol* and *env* genes) (18) (Fig. 4). The cells were selected for Hyg^r, and the resistant cells were pooled and designated STEP 1 cells (Fig. 4, STEP 1). Virus from step 1 cells was used to infect the MLV helper cell line PG13. Infected cells were selected for Hyg^r, and individual clones were isolated and designated STEP 2 cells (Fig. 4, STEP 2). The structures of the proviruses formed from the SNV U3-minus vector in the PG13 cells were monitored by Southern (DNA) analysis. The *Xho*I linker in JZ446 is duplicated in the 5′ LTR during formation of the STEP 2 provirus (5). The STEP 2 clones containing the expected *Xho*I fragment that hybridized to a *hyg* probe were used for further analysis (Fig. 4, STEP 2). To test whether any virus capable of forming Hyg^r colonies was produced by the STEP 2 cells, the supernatant medium (4 ml) from each STEP 2 cell clone was used to infect D17 cells, and the infected cells were selected for Hyg^r. No Hyg^r colonies were detected. This was because the deletion of the U3 region (promoter and enhancer) in the SNV 5′ LTR prevented transcription from the SNV vector (4). The infectious MLV vectors LN, LN290, L290N, L290N290, and LN80 (Fig. 4) were each transfected into the amphotropic helper cell line PA317 (11) (Fig. 4). Viruses from the transfected PA317 cells were used to superinfect the STEP 2 cells containing JZ446 or JZ211, and the infected cells were selected for neomycin resistance (Neo^r). Individual Neo^r clones were isolated and designated STEP 3 cells (Fig. 4, STEP 3). Each STEP 3 cell clone contained a single JZ446 or JZ211 integration and a single integration of LN, LN80, LN290, L290N, or L290N290.

Introduction of a single JZ525 and a single YM2 into helper cell line PG13. Plasmid DNA of pJZ525 (Fig. 5A) was transfected into the MLV amphotropic helper cell line PA317 (11). Virus from transfected PA317 cells was used to infect the MLV xenotropic helper cell line PG13 (12). Infected cells were selected for Hyg^r, and individual Hyg^r green clones were isolated and designated STEP 2 cells. Plasmid DNA of pYM2 was used to transfect fresh PA317 cells. Transfected PA317 cells were selected for Neo^r. The green Neo^r cells were sorted by flow cytometry. Viruses released from green cells were used to infect STEP 2 cells, which contained JZ525 proviruses. Infected STEP 2 cells were selected for

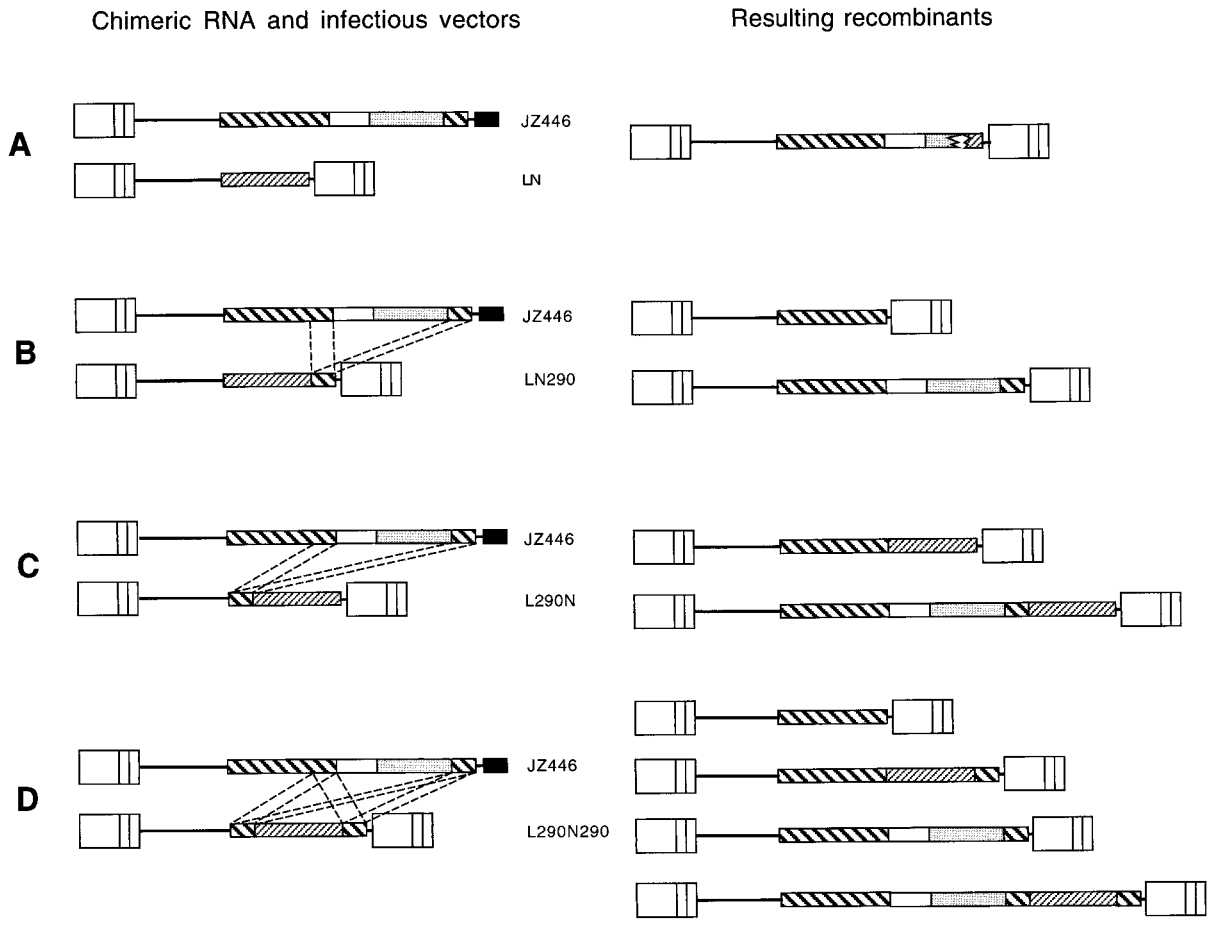

FIG. 3. Chimeric RNA vector JZ446, infectious virus vectors, and resulting recombinants. JZ446 is identical to JZ211 (Fig. 2) except that it also includes *gfp* and an insertion of a second identical sequence homologous to 290 bp of the 3′ *hyg* sequence into the 3′ untranslated portion of *gfp* (downstream of *gfp* or after the *gfp* stop codon). After one round of replication, the JZ446 recombinants showed that the downstream 3′ *hyg* sequence had recombined with the upstream *hyg* sequence, resulting in a deletion of *gfp*. These recombinants, therefore, are clear under a fluorescence microscopy.

Neo^r, and individual Neo^r cells were cloned. Due to the high rate of recombination between the two IRESs within YM2, the *gfp* gene between the two IRESs was deleted in a large portion of Neo^r cells. To distinguish between the Neo^r PG13 cells containing parental and recombinant YM2, the cellular DNAs of each Neo^r colony were digested with *Eco*RV and hybridized with a *hyg* probe. Neo^r cells integrated with a parental YM2 generated a 5.5-kb fragment, while cells with a recombinant YM2 generated a 4.1-kb fragment. The Neo^r cells with a parental YM2 were designated STEP 3 cells and used for further study.

Cells, transfection, and infection. The handling of D17 cells (a dog osteosarcoma cell line; ATCC CRL-8468), PA317 cells (ATCC CRL-9078), and PG13 helper cells (ATCC CRL-10686), DNA transfections, virus harvesting, and virus infections were as previously described (22).

Fusion of D17 cells and PG13 cells. The cells (5×10^5 cells of each cell line) were fused with polyethylene glycol 1500 (PEG). The cells were mixed in 1 ml of Dulbecco modified Eagle medium (DMEM) with 10% of PEG and 5% dimethyl sulfoxide for 3 min. PEG was diluted by adding 5 ml (DMEM), and cells were plated in a 60-mm dish and incubated at 37°C. The PEG medium was replaced with fresh DMEM containing 10% fetal calf serum 1 h after fusion. Viruses were collected 36 h after fusion.

Sequence analyses of junctions of recombinants between JZ446 and LN80. Cellular DNAs of STEP 4 D17 cells were isolated and amplified by PCR using primer 5′-CTACTTCGAGCGGAGGCATCC-3′, which hybridized within the 5′ end of *hyg*, and 5′-ATGCCTTGCAAAATGG-3′, which hybridized to the U3 region of the 3′ LTR (Fig. 6C and D). Primers 5′-GCGCGGCCGTCTGGAC-3′, 5′-CTGGAGTTCGTGACCG-3′, and/or 5′-CTTAAGCTAGCTTGCC-3′ were used for sequencing the amplified fragments.

Fluorescence microscopy. A fluorescence inverted microscope (Zeiss Axiovert 25) with a 100-W mercury arc lamp and a fluorescent filter set (CZ909) consisting of a 470/40-nm exciter, a 515-nm emitter, and a 500-nm beam splitter were used to detect GFP in living cells.

RESULTS

Direct evidence for intramolecular recombination. Previous study demonstrated that the rate of recombinations between two identical sequences within the same RNA molecules was about 62% during a single replication cycle (19) (Fig. 1A). However, the high rate of recombination could be either intra- or intermolecular, because it could result from an intramolecular event or from the recombination of a downstream sequence of one RNA molecule with the upstream sequence of the other RNA molecule.

To demonstrate an intramolecular event, chimeric RNA vector JZ446 (Fig. 1BC) was introduced into the MLV helper cell line PG13 as described in the Materials and Methods JZ446, derived from SNV, contained a deletion in the U3 region of the 3′ SNV LTR. (Fig. 4, top). This vector also contained a truncated MLV vector between the two SNV

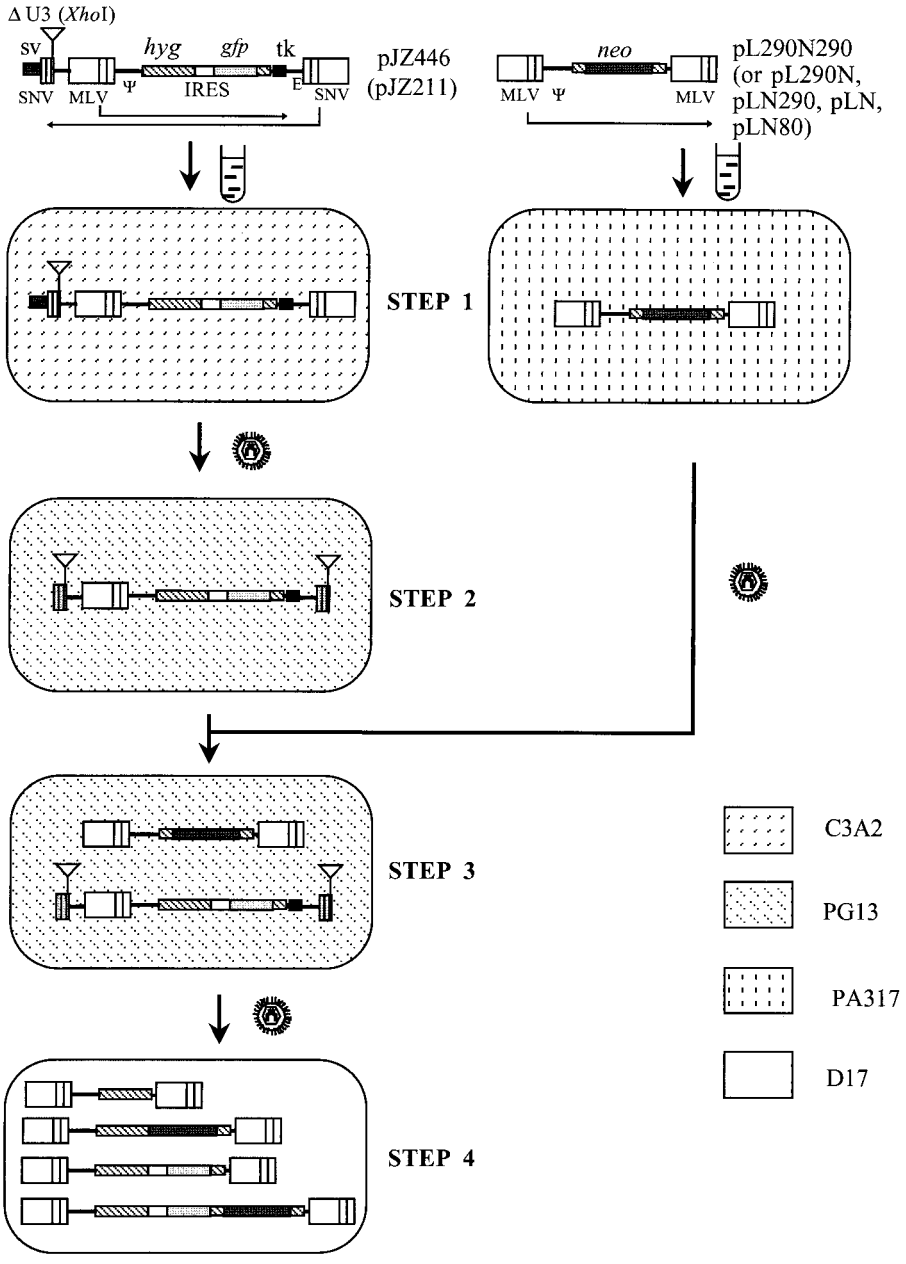

FIG. 4. Outline of an experimental approach for determining the rate of recombination during a single cycle of retroviral replication between the chimeric RNA vector JZ446 (or JZ211) and infectious vectors. Plasmid backbone sequences are not shown. Directions of transcription in SNV and MLV are shown by long thin arrows. Transfections are indicated by test tube shapes. Infections are indicated by virion shapes. The different backgrounds represent the indicated cell lines. SV, late polyadenylation signal of simian virus 40; Ψ and E, encapsidation sequences of MLV and SNV, respectively; tk, thymidine kinase. The lines in the LTR separate the U3, R, and U5 regions.

LTRs, in a transcriptional orientation opposite that of the SNV LTRs. In this truncated MLV vector, *hyg* was expressed from the 5′ MLV LTR, and an HSV TK poly (A) addition signal replaced the deleted 3′ MLV LTR. This truncated MLV vector contained *hyg* and *gfp*, separated by an IRES sequence. *hyg* was expressed from the 5′ MLV LTR, while *gfp* was expressed from the IRES sequence. The IRES was isolated from an encephalomyocarditis virus origin and allows the ribosome to bind to the internal AUG that initiates translation of the second gene independently from the upstream gene (1, 2). Cells that express the *gfp* gene are green under a fluorescence microscope, while cells without the *gfp* gene product are clear (16, 19). In addition, the MLV sequences of JZ446 also included the insertion of a second sequence homologous to 290 bp of the 3′ end of *hyg* inserted into the 3′ untranslated portion of *gfp* (Fig. 1B and C). As expected, after one round of replication, the JZ446 recombinants showed that the downstream 3′ *hyg* sequence had recombined with the upstream *hyg* sequence, resulting in a deletion of *gfp* (Fig. 6D). Therefore, these recombinants are clear under a fluorescence microscope.

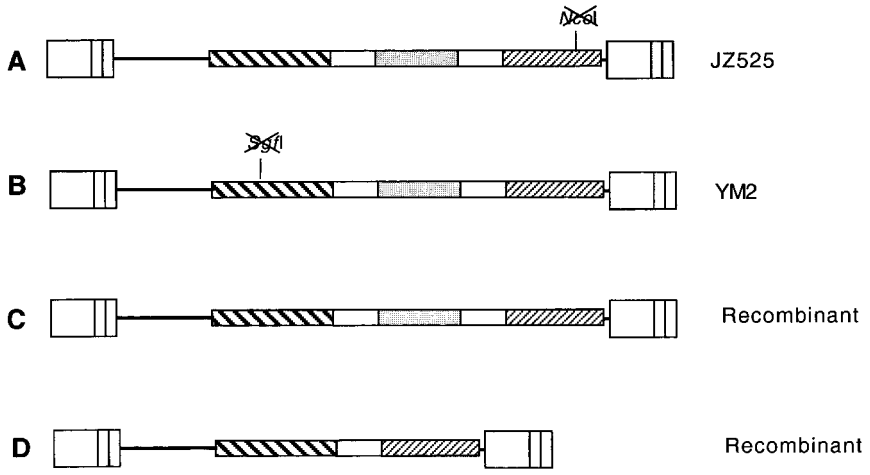

FIG. 5. Structures of retrovirus vectors used to determine the rate of intramolecular recombination. (A) Structure of a retroviral vector encoding a frameshift mutation within *neo*. JZ525 contains, from 5′ to 3′, *hyg*, an IRES sequence, *gfp*, an additional copy of the IRES sequence, and *neo*. The *neo* gene encoded a frameshift mutation at its *Nco*I site and thus was nonfunctional. (B) Structure of a retroviral vector encoding a frameshift mutation in *hyg*. YM2 was identical to JZ525 except that *neo* was functional but *hyg* was nonfunctional because of a frameshift mutation at the *Sgf*I site within the *hyg* open reading frame. (C) Recombinant of JZ525 and YM2. This recombinant encodes functional *hyg, neo*, and *gfp*. (D) Recombinant of JZ525 and YM2. This recombinant is identical to C except that the *gfp* gene between the two IRES sequences is deleted.

Next, the chimeric RNA vector JZ446 and infectious vectors LN and LN80 were separately introduced into the helper cell line PG13 (12) as described in Materials and Methods. Individual clones were designated STEP 3 cells (Fig. 4, STEP 3). Viruses from each STEP 3 clone were used to infect D17 cells, and the infected cells were selected separately for Hyg^r and for Neo^r. The resulting cells were designated STEP 4 cells (Fig. 4, STEP 4). With this approach, Hyg^r colonies form only when a recombination between the JZ446 and LN or LN80 vectors has occurred so that *hyg* is flanked by two LTRs. The target cells do not contain viral *gag-pol* and *env* gene products for retrovirus replication. Therefore, progeny virus cannot be released from them (22). Consequently, these vector viruses have undergone only one cycle of replication.

Since the STEP 4 resulted from selection for Hyg^r, the LN 3′ LTR had to recombine with the sequence downstream of *hyg* within JZ446. This recombination was nonhomologous because the 3′ end of JZ446 did not contain any sequence identical to LN. Therefore, formation of a Hyg^r colony resulted from a nonhomologous recombination between JZ446 and LN.

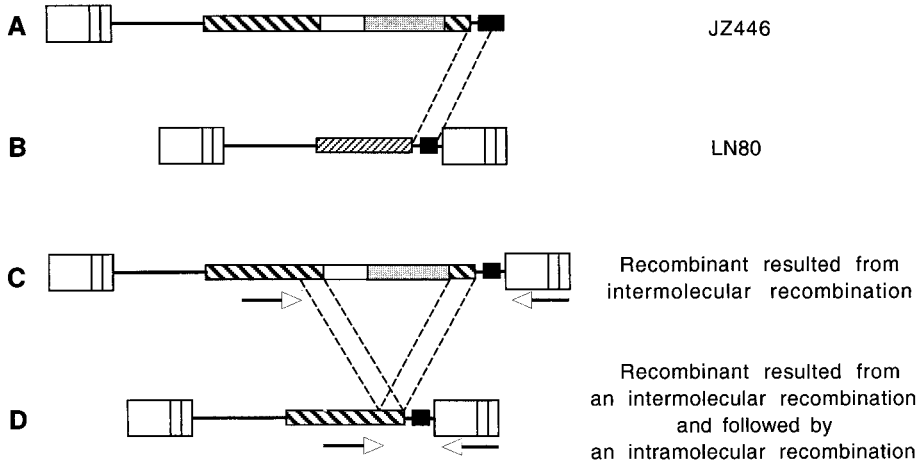

FIG. 6. An intramolecular recombination follows an intermolecular recombination. (A) The RNA chimeric virus JZ446 contains only one LTR and *hyg*. Hyg^r colonies form only when recombination between JZ446 and an infectious vector occurs so that *hyg* is flanked by two LTRs. (B) Infectious MLV vector LN80 containing an 80-bp sequence identical to the TK sequence in JZ446. The 80-bp sequence was inserted into the 3′ portion of the *neo* sequence (downstream of the 3′ *neo* gene or after the *neo* stop codon). Most of the recombinants utilized the 80-bp sequences identical between JZ446 and LN80. (C) Recombinants between JZ446 and LN80. The 80-bp TK sequence is located at the 3′ end downstream of the second 3′ *hyg* sequence. Recombinants resulted from intermolecular recombination between the identical 80-bp sequences within JZ446 and LN80 and contained two 290-bp 3′ *hyg* sequences with *gfp* between within the same RNA molecule. The arrowheads represent locations of the PCR primers. (D) Recombinants resulting from an intramolecular recombination following an intermolecular recombination. Recombination between the two identical 290-bp sequences within JZ446 formed a clear Hyg^r colony by deletion of *gfp*.

TABLE 1. Assay of D17 cells infected with STEP 3 clones of PG13 cells containing JZ446 and an infectious LN- or LN80-based vector

Clone	Titer of viruses selected for:		Rate[a] (10^{-5})	No. of clones that were:	
	Hyg^r	Neo^r (10^5)		Clear	Green
JZ446/LN 1-1	9.3	2.95	3.16	61	1
JZ446/LN 1-2	12.3	2.88	4.28	69	3
JZ446/LN 1-3	8.3	2.80	2.98	38	0
JZ446/LN 2-1	8.0	3.60	2.22	46	4
JZ446/LN 2-3	3.7	3.35	1.09	13	1
JZ446/LN 7-1	6.0	26.7	0.22	47	2
JZ446/LN 7-3	7.0	1.57	4.46	46	2
JZ446/LN80 1-1	240	14.5	16.6	101	27
JZ446/LN80 1-2	265	10.3	25.7	116	19
JZ446/LN80 1-3	910	12.1	75.2	198	38
JZ446/LN80 1-4	88	6.4	137	189	27
JZ446/LN80 2-1	139	9.6	14.5	27	4
JZ446/LN80 2-2	184	11	16.7	72	11
JZ446/LN80 2-3	45	0.68	66	20	4
JZ446/LN80 7-1	137	8.1	16.9	50	7
JZ446/LN80 7-3	39	0.52	75	35	3
JZ446/LN80 7-4	225	5.4	41.7	132	11

[a] Rate of recombination between JZ446 and infectious vectors, expressed as the ratio of Hyg^r titer to Neo^r titer. The average rate of recombination between JZ446 and LN is $7.8 \times 10^{-5} \pm 2.7 \times 10^{-5}$, while the average rate between JZ446 and LN80 is $48.6 \times 10^{-5} \pm 39.9 \times 10^{-5}$. The rate of deletion of the *gfp* gene is the ratio of the number of clear colonies to the number of total colonies (sum of the number of clear and green colonies). The rate of deletion for JZ446 and LN is 96%, while the rate of deletion for JZ446 and LN80 is 86%.

The ratio of the Hyg^r titer to the Neo^r titer represented the rate of recombination between the JZ446 and LN, which was $7.8 \times 10^{-5} \pm 2.7 \times 10^{-5}$ (Table 1). This result was consistent with previous report that the rates of nonhomologous recombinations were very low (21).

The second infectious MLV vector, LN80 (Fig. 1C), was identical to LN except that an 80-bp HSV TK sequence before the poly(A) addition site (or AATAAA) was inserted into the 3′ untranslated portion of the *neo* sequence. This 80-bp TK sequence is identical to the TK sequences within JZ446 (Fig. 1C). Since there was an 80-bp sequence homology between JZ446 and LN80, most recombinations between the two vectors utilized the 80-bp sequences. The rate of recombination for vectors containing shared homologous sequences is higher than the rate of nonhomologous recombination (22, 23). The rate of recombination ($48.6 \times 10^{-5} \pm 39.9 \times 10^{-5}$) between JZ446 and LN80 was approximately six times that between JZ446 and LN ($7.8 \times 10^{-5} \pm 2.7 \times 10^{-5}$) (Table 1); i.e., only 16% (7.8/48.6) of recombinations between JZ446 and LN80 resulted from nonhomologous recombination.

Two crossovers may occur to form clear Hyg^r LN80 colonies (Fig. 6). First, most recombinations between JZ446 and LN80 resulted from recombination between the two identical 80-bp TK sequences such that *hyg* was flanked by two LTRs (Fig. 6A and B). Recombinants resulting from the first intermolecular recombination contained two 290-bp 3′ *hyg* sequences flanking *gfp* within the same RNA molecule (Fig. 6C). The second event would be an intramolecular crossover between the two identical 290-bp sequences within JZ446 to delete *gfp* and form a clear Hyg^r colony (Fig. 6D). If this intramolecular recombination did not follow the intermolecular recombination, a green Hyg^r colony would be formed (Fig. 6C).

Recombination between JZ446 and LN80 occurred at the shared 80-bp homologous TK sequence, as well as at nonhomologous sequences. As mentioned above, there was approximately 84% (100% − 16%) homologous recombinations between JZ446 and LN80 which utilized the 80-bp sequences identical between the two vectors. Only 14% of the Hyg^r colonies for JZ446 and LN80 examined by fluorescence microscopy were green, while 86% of colonies were clear (Table 1). Most green colonies were assumed to represent recombinants between LN80 and JZ446 within the 80-bp sequences without further recombinations (Fig. 1C). Clear colonies (86%) represented the sum of the numbers of nonhomologous recombination between the LN80 and upstream sequences of the *gfp* gene of JZ446 and the numbers of homologous recombination between the two 80-bp sequences within the two vectors plus a second intramolecular recombination between the two 290-bp sequences within JZ446 (Fig. 6D), which was more than 70% (86% − 16%). In other words, 70% of the total 84% recombinants utilizing the 80-bp TK homologous sequences had further undergone an intramolecular recombination (Fig. 6C and D). Therefore, in this case, the rate of intramolecular recombination was approximately 83% (70%/84%).

Since most green recombinants resulted from a recombination between the two shared 80-bp sequences within JZ446 and LN80, the RNAs transcribed from those green recombinant proviruses with two identical 290-bp sequences should undergo recombination if the RNAs were reverse transcribed. To determine the phenotypic nature of green recombinants between JZ446 and LN80, the green STEP 4 D17 cells (Fig. 6C) and fresh PG13 cells were fused as described in Materials and Methods. The MLV proteins (Gag-Pol and Env) from PG13 helper cells packaged the viral RNA transcribed from the green provirus (Fig. 6C) in the STEP 4 D17 cells. Viruses released from the fused cells were used to infect fresh D17 cells. The infected D17 cells were selected for Hyg^r. Five of six STEP 4 clones analyzed produced viruses after fusing with PG13 cells. The titers of those viruses ranged from 300 to 3,000 CFU/ml. The Hyg^r colonies were examined under a fluorescence microscope. The ratio of the number of the clear colonies to the number of total colonies represented the rate of recombination between the two 290-bp sequences. The rate was 59% ± 5%, which was similar to the rate for JZ442 + 3′ Hyg (62% ± 9%) (Fig. 1A) (19).

To determine the genomic structure of recombinants of JZ446 and LN80, proviral sequences of the STEP 4 cells were analyzed. Cellular DNAs were isolated from individual Hyg^r STEP 4 green and clear clones and were amplified by PCR using two primers hybridized within the MLV proviruses as described in Materials and Methods. The amplified proviral DNAs were sequenced. All four green colonies analyzed coincided with the structure predicted in Fig. 6C, which encoded, from 5′ to 3′, the *gfp* sequence and the 290-bp sequence from JZ446, the 80-bp shared TK sequence, and the U3 region from LN80. All 10 clear colonies analyzed were the structure predicted in Fig. 6D, which encoded the *hyg* sequence from JZ446, the shared 80-bp sequence, and the U3 region from LN80. The high rate of recombination must occur during reverse transcription, because the deletion rate after reverse transcription

is very low (less than 10^{-5}) (9). Therefore, intramolecular recombination actually occurred between the two 290-bp sequences within JZ446.

High rates of recombination between two identical sequences within the same RNA molecule resulted mostly from intramolecular recombination. We have provided evidence that intramolecular recombination actually occurred within the chimeric RNA vector JZ446. The high rate of recombination, however, might result from a negative interference since the intramolecular recombinations within JZ446 followed an intermolecular recombination between the two vectors. The above observation demonstrated that intramolecular recombinations occurred, but we could not determine whether the high rate of recombination of two identical sequences (Fig. 1A) (19) resulted mostly from intramolecular recombination.

Previous work indicated that the recombination (both inter- and intramolecular) rate between two identical sequences within the same retroviral RNA molecule is 62% per replication cycle (Fig. 1A) (19). The intermolecular recombination rate between a 1-kb homologous sequence is only 4% (6). If the high rate (62%) of recombination between the two identical sequences resulted from intermolecular recombinations, it would be expected that the presence of four copies of identical 290-bp sequences within the two RNA molecules would result in a significantly higher rate of intermolecular recombination. To separate intermolecular from intramolecular recombination, chimeric RNA vectors JZ211 and JZ446 (Fig. 2 and 3) were introduced into the MLV helper cell line PG13 as described above. JZ211 has been described previously (22). Briefly, JZ211 was identical to JZ446 (Fig. 2 and top of Fig. 4) except that it carried only *hyg* and thus contained only one copy of the 290-bp 3′ *hyg* sequence. As described above, JZ446 contained two copies of the 290-bp sequences. Infectious vectors were used to recombine with JZ211 and JZ446. In addition to LN described above, three infectious vectors were constructed. LN290 (Fig. 2B and 3B) and L290N (Fig. 2C and 3C) contained a *neo* gene and one copy of the 290-bp sequence from the 3′ end of the *hyg* gene, except that the 290-bp sequence of LN290 was inserted into the 3′ end of *neo* and served as the 3′ untranslated sequence, whereas the 290-bp sequence of L290 was inserted into the 5′ end of *neo* and served as the 5′ untranslated sequence. L290N290 contained two copies of the 290-bp sequence (Fig. 2D and 3D).

Next, the chimeric RNA vectors JZ211 (and JZ446) and infectious vectors LN, LN290, L290N, and L290N290 were separately introduced into the helper cell line PG13 (12) as described in Materials and Methods. Individual clones were designated STEP 3 cells (Fig. 4, STEP 3). Viruses from each STEP 3 clone were used to infect D17 cells, and the infected cells were selected separately for Hyg^r and for Neo^r. The resulting cells were designated STEP 4 cells (Fig. 4, STEP 4). With this approach, Hyg^r colonies form only when a recombination between JZ211 (or JZ446) and any one of LN290, L290N, and L290N290 vectors has occurred at the shared 290-bp homologous sequences so that the *hyg* gene is flanked by two LTRs.

If a nonhomologous recombination event occurs between JZ211 (or JZ446) and LN, it results in a Hyg^r colony. The rate of recombination is much lower than the rates for vectors containing the shared 290-bp homologous sequences (Fig. 2A and 3A; Table 2) (22, 23); therefore, most recombinations were between the 290-bp sequences. The ratios of Hyg^r CFU to Neo^r CFU produced were $170 \times 10^{-5} \pm 50 \times 10^{-5}$ and $80 \times 10^{-5} \pm 60 \times 10^{-5}$ for LN290 and L290N, respectively, as described previously (19) (Table 2; Fig. 2B and C). Those ratios represented the rate of recombination between one copy of the 290-bp within the chimeric RNA vector (JZ211) and one copy of the 290-bp sequence within the infectious vector (L290N or LN290). L290N290 contained two copies of the 290-bp sequences identical to that in JZ446. Specifically, the 290-bp 3′ *hyg* sequence was inserted both upstream and downstream of *neo* within this vector (Fig. 2D and 3D). The actual titers of the infectious viruses (L290N290) as measured by Neo^r selection should be higher than that. This difference could be due to a recombination between the two identical sequences on either side of the *neo* gene of L290N290 that would result in a deletion of *neo*. To estimate the rate of deletion within L290N290 during a single round of replication, STEP 3 viruses of L290N290 were used to infect D17 cells. Infected cells were pooled without selection, and the DNAs of pooled D17 cells were digested with *Eco*RV and hybridized with a probe containing the MLV packaging signal. *Eco*RV digested within the LTRs of the vectors such that LN290 pro-

TABLE 2. Assay of D17 cells infected with STEP 3 clones of PG13 cells containing JZ446 and an infectious LN290- or 290LN-based vector

Clone	Titer of viruses selected for:		Rate[a] (10^{-5})	No. of clones that were:	
	Hyg^r	Neo^r (10^5)		Clear	Green
JZ446/LN290 1-1	420	2.38	176	46	5
JZ446/LN290 1-2	763	4.43	172	86	3
JZ446/LN290 1-3	600	1.60	375	138	5
JZ446/LN290 2-1	683	5.03	136	158	4
JZ446/LN290 2-2	240	2.97	80.8	39	3
JZ446/LN290 2-3	450	4.80	93.8	52	5
JZ446/LN290-7-1	500	6.52	76.7	133	5
JZ446/LN290 7-2	180	2.15	83.7	51	0
JZ446/LN290-7-3	217	11.2	19.3	56	4
JZ446/290LN 1-1	167	1.73	96.3	23	0
JZ446/290LN 1-2	483	3.87	125	67	1
JZ446/290LN 2-1	89.3	1.22	73.2	233	9
JZ446/290LN 2-2	85	1.50	56.7	207	7
JZ446/290LN 2-3	136	2.90	46.9	195	8
JZ446/290LN-7-1	61.3	1.73	35.4	139	7
JZ446/290LN 7-2	70	3.90	17.9	133	6
JZ446/290LN-7-3	46.3	2.57	18.0	111	6
JZ446/290LN290 1-1	1,770	2.18	812	141	6
JZ446/290LN290 1-2	116	0.30	387	242	10
JZ446/290LN290 1-3	590	0.47	1255	125	9
JZ446/290LN290 2-1	1,130	2.10	538	266	25
JZ446/290LN290 2-2	220	1.27	173	28	0
JZ446/290LN290 2-3	263	0.53	497	38	2
JZ446/290LN290-7-1	413	1.23	336	98	5
JZ446/290LN290 7-2	587	0.95	618	146	13
JZ446/290LN290-7-3	14.3	0.18	79.4	40	2

[a] The rates of recombinations between JZ211 and infectious vector were described previously (19). The rate of recombination between JZ211 and LN is $3 \times 10^{-5} \pm 2 \times 10^{-5}$. The rate of recombination between JZ211 and LN290 is $170 \times 10^{-5} \pm 50 \times 10^{-5}$. The rate of recombination between JZ211 and L290N is $80 \times 10^{-5} \pm 60 \times 10^{-5}$. The rate of recombination between JZ211 and L290N290 is $600 \times 10^{-5} \pm 130 \times 10^{-5}$. The rate of recombination between JZ446 and LN290 is $140 \times 10^{-5} \pm 100 \times 10^{-5}$. The rate of recombination between JZ446 and LN290 is $59 \times 10^{-5} \pm 38 \times 10^{-5}$. The rate of recombination between JZ446 and LN290 is $520 \times 10^{-5} \pm 360 \times 10^{-5}$ (or $520 \times 5/6 = 430$).

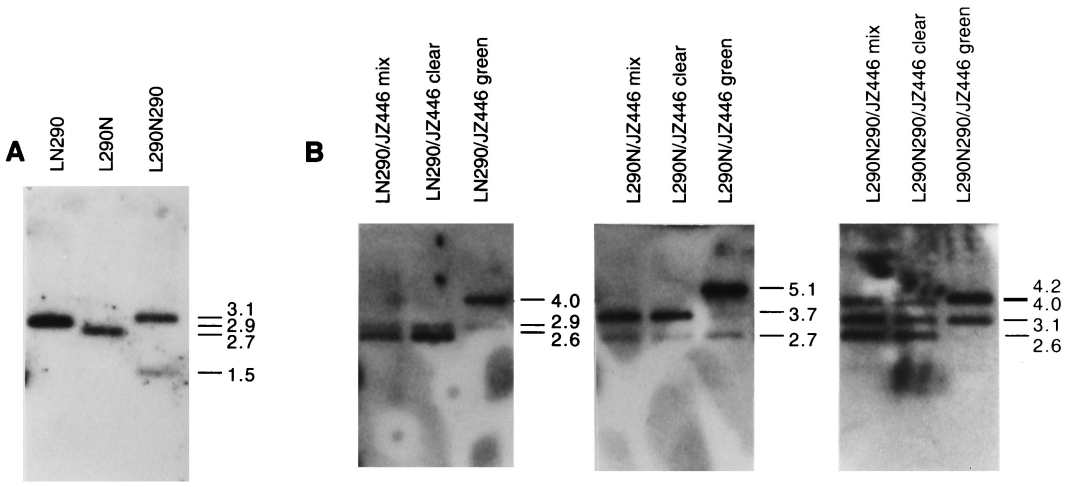

FIG. 7. Southern analyses of recombinants between JZ446 and LN290, L290N, and L290N290. (A) Southern analysis of chromosomal DNA of unselected STEP 4 cells. Cellular DNAs were isolated from JZ446/L290N290 STEP 4 cells, digested with *Eco*RV, and hybridized with a package signal probe. (B) Southern analysis of chromosomal DNA of Hyg^r STEP 4 cells. Cellular DNAs were isolated from STEP 4 cells (Fig. 4) that had been pooled from Hyg^r colonies; the DNA was then digested with *Eco*RV and hybridized with a *hyg* probe (Fig. 3). The cells examined are listed above the lanes. Molecular sizes (kilobase pairs) are shown on the right. The additional fragment (2.9 kb) in JZ446/LN290 proviruses was an *Eco*RV fragment of LN290 which contains a 290-bp 3′ *hyg* sequence. The additional 2.7-kb *Eco*RV fragment of L290N and 3.1-kb *Eco*RV fragment of L290N290 also resulted from the infectious viruses.

duced a 2.9-kb fragment and L290N produced a 2.7-kb fragment (Fig. 7A). The parental provirus of L290N290 produced a 3.1-kb fragment, while the recombinant provirus with the *neo* deletion produced a 1.5-kb fragment (Fig. 7A). The ratio of the intensity of the 3.1-kb fragment and the 1.5-kb fragment was about 5. After normalization of the L290N290 titer, the JZ446/L290N290 recombination rate was 430×10^{-5} (Fig. 3D) (Table 2). Intermolecular recombination between JZ446 and L290N290 (i.e., two RNA molecules that together have four copies of the identical 290-kb sequences) increased only three to six times above that of intermolecular recombinations between JZ211 and LN290 or L290N (i.e., two RNA molecules that together have two copies of the 290-kb identical sequences). The recombination rate between two identical sequences within the same RNA molecules (i.e., two RNA molecules containing four copies of the 290-kb identical sequences) was 62%, (19), while the rate of the intermolecular recombination between two 290-bp homologous sequences (i.e., two RNA molecules containing two copies of the 290-kb identical sequences) should be 1.16% (290/1,000 × 4%) (6). The recombination rate between the two identical sequences within the same RNA molecule would increase 50-fold. Therefore, this observation suggested that the high rate of recombinations between two identical sequences within the same RNA molecule resulted mostly from intramolecular recombination.

To determine whether recombinations had occurred at the 5′ or the 3′ end of the 290-bp *hyg* sequence, the DNA from STEP 4 cells was digested with *Eco*RV and hybridized with a *hyg* probe. The proviruses resulting from recombination between JZ446 and L290N290 using the upstream and downstream *hyg* sequence gave four different-sized *Eco*RV fragments that hybridized with a *hyg* probe (Fig. 7B). The clear recombinants (92% of total Hyg^r colonies) utilizing the upstream *hyg* sequence of L290N290 gave a 4.0-kb *Eco*RV fragment, and those utilizing the downstream *hyg* sequence gave a 2.6-kb *Eco*RV fragment. The green recombinants (8% of total Hyg^r colonies) utilizing the upstream *hyg* sequence of L290N290 gave a 5.7-kb *Eco*RV fragment, while those utilizing the downstream *hyg* sequence gave a 4.2-kb *Eco*RV *hyg* fragment. The results shown in Fig. 7B indicate that both identical sequences were used to form recombinants between the chimeric RNA and the infectious vector.

Determination of the rate of intramolecular recombination. Evidence for intramolecular recombination provided above was based on assays using two heterologous RNA molecules. The packaging and arrangement of the two different RNA molecules within a viral particle may be very different from those of two homologous RNA molecules. To determine the rate of intramolecular recombination, two homologous MLV-based vectors were constructed. The first vector, JZ525, carries, from 5′ to 3′, *hyg*, an IRES sequence, *gfp*, an additional copy of the IRES sequence, and *neo* (Fig. 5A). In this vector, *hyg* was expressed from the 5′-end LTR, and *gfp* and *neo* were expressed from two IRESs. The *gfp* gene was flanked by the two identical IRES sequences. After one round of replication, recombination between the two IRES sequences would delete the *gfp* gene (Fig. 5D), so that cells encoding the parental JZ525 were green under a fluorescence microscope whereas cells with the recombinant JZ525 were clear (Fig. 5D). The *neo* gene encoded a frameshift mutation at its *Nco*I site so that the *neo* gene was nonfunctional within this vector. Cells infected with JZ525 were Hyg^r and Neo^s. The second vector, YM2, was identical to JZ525 except that *neo* was functional but *hyg* was nonfunctional because of a frameshift mutation on the *Sgt*I site within the *hyg* open reading frame (Fig. 5B). As a result, cells containing YM2 were Hyg^s and Neo^r. JZ525 and YM2 were introduced into the PG13 cell line as described in Materials and Methods. Approximately half of the viruses released from these cells would contain a JZ525 RNA molecule and a YM2 RNA molecule. (Retroviruses package two RNA molecules in

TABLE 3. Assay of STEP 3 clones[a] on D17 cells

Clone	Neo^r			Hyg^r			Neo^r Hyg^r			Rate[b] (%)
	Titer (10^3)	No. that were:		Titer (10^3)	No. that were:		Titer (10^3)	No. that were:		
		Clear	Green		Clear	Green		Clear	Green	
1-4	135	58	51	27.5	22	16	0.35	96	134	0.4
3-1	137	47	57	36.5	20	29	1.00	57	107	1.2
4-2	110	36	33	23	24	38	1.10	32	82	1.7
4-4	101	30	28	26	137	164	1.05	112	172	1.7

[a] Each clone was an individual clone of PG13 cells containing a single JZ525 and a single YM2. Viruses released from each clone were used to infect D17 cells. Infected D17 cells were selected for Neo^r, Hyg^r, and Neo^r/Hyg^r, respectively.

[b] The rate of recombination between JZ525 and YM2 is twofold above the ratio of double-resistant titer to the sum of two single-resistant titers. The average rate of recombination is 1.3% ± 0.6%. The rate of deletion of the *gfp* gene is the ratio of the number of clear colonies to the number of the total colonies. The rate of deletion of Neo^r colonies is 51% ± 4%. The rate of deletion of Hyg^r colonies is 46% ± 9%. The rate of deletion of Neo^r Hyg^r colonies is 36% ± 6%.

each virion.) Retroviral recombinations occur during minus-strand DNA synthesis, which begins from the 3′ end of the viral RNA molecules (20). An intermolecular recombination occurring between the downstream IRES within YM2 and the upstream IRES within JZ525 would not only delete *gfp* but also form a double-resistant (Hyg^r Neo^r) provirus. Only half of the intermolecular recombinations would result in double resistance, while the other half would result in double-sensitive proviruses which could not be detected after selection. Therefore, the intermolecular recombination rate should be twice the ratio of the number of the double-resistant colonies to the number of the single-resistant colonies. Most intramolecular recombination between the two identical IRES sequences would form a single-resistant provirus without *gfp*.

Viruses released from the helper cell line PG13 containing JZ525 and YM2 were used to infect D17 cells. Infected cells were selected for Hyg^r, Neo^r, and Hyg^r Neo^r. The rate of recombinations between the two vectors should be twofold above the ratio of the number of the double-resistant colonies to the sum of two single-resistant colonies. The recombination rate between the two frameshift mutations was 1.3% ± 0.6% (Table 3).

The rate of recombination between the two IRES sequence resulting in *gfp* deletion would be the ratio of the number of clear colonies to the number of total single-resistant colonies, which was 46 to 51% or 48.5% on average (Table 3). The rate of intermolecular recombination between a downstream IRES within one vector and the upstream IRES within the other vector was the product of the rate of intermolecular recombination (1.3%) and the deletion rate of the double-resistant colonies (36% [Table 3]), which was only 0.5% (1.3% × 36%). Therefore, approximately 99% [(48.5% − 0.5%)/48.5%] of recombinations between the two identical sequences resulted from an intramolecular recombination.

To determine whether recombinations occurred between the two identical IRES sequences within JZ525 and YM2, DNA from STEP 4 cells was digested with *Eco*RV and hybridized with a *hyg* probe. The green proviruses produced a 5.5-kb fragment, and the clear proviruses produced a 4.1-kb fragment. The results shown in Fig. 8 indicate that the clear clones resulted from recombinations between the two identical IRES sequences within JZ446 and YM2.

DISCUSSION

Retroviruses, as a consequence of having two RNA molecules in their virions, recombine at a high rate. The rate of recombination between two identical sequences within the same RNA molecule is about 62% (19). It was deduced that recombination may occur between two sequences on one RNA molecule (intramolecular) as well as between the two RNA molecules (intermolecular) (17). We demonstrated intramolecular recombination occurred within the chimeric RNA vector JZ446. Using two homologous vectors, we determined that approximate 99% recombinations between the two identical sequences within the same RNA molecules resulted from an intramolecular recombination.

The rate of intramolecular recombination (83%) within JZ446 (Fig. 6) is higher than the rate of deletion (62%) between the same 290-bp sequence identities within each of two essentially homologous RNA molecules (JZ442 + 3′ Hyg) (Fig. 1A). The deletion within the two homologous RNA molecules requires only one step of recombination: either an intramolecular or an intermolecular recombination between the downstream sequence from one RNA molecule and the upstream sequence of the same or the other RNA molecule. However, the deletion within the same two 290-bp sequences within the chimeric RNA molecule (JZ446) requires two steps. The first step is intermolecular, allowing *hyg* to be located

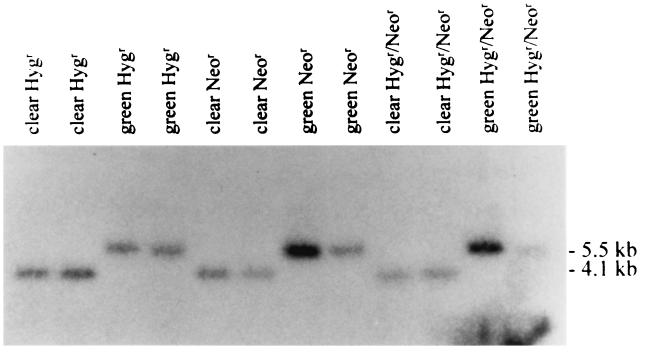

FIG. 8. Southern analysis of recombinants between JZ425 and YM2. Cellular DNAs from green or clear Hyg^r, Neo^r, and Hyg^r Neo^r STEP 4 clones were digested with *Eco*RV and hybridized with a *hyg* probe. The clones examined are listed above the lanes. Molecular sizes (kilobase pairs) are shown on the right.

between two LTRs; the second step is intramolecular, deleting *gfp*. The discrepancy may have resulted from negative genetic interference.

We hypothesized that the rate of intramolecular would be higher if it followed an intermolecular recombination. However, the rate of deletion within JZ525/YM2 with an intermolecular recombination was a little bit lower than that without an intermolecular recombination (Table 3). Retroviral recombination occurs during minus-strand DNA synthesis (20), and so a minus-strand DNA from downstream sequences lands on an upstream sequence of the RNA template. The difference between JZ446/LN and JZ525/YM2 is that in the former system, the two identical sequences were available within JZ446 after an intermolecular recombination (Fig. 6C). However, in the latter system, as soon as reverse transcription passed the downstream IRES, the intramolecular recombination between the two identical sequences (IRESs) could not occur. In this system, intermolecular recombinants between the two frameshift mutations (*Sgf*I and *Nco*I) were selected (Fig. 5A and B). In JZ525/YM2, the *hyg* sequence downstream of the *Sgf*I site, the upstream IRES, and the *gfp* gene were 2 kb in length, while the downstream IRES and the *Nco*I site upstream of the *neo* sequence were only 1 kb in length. The difference in the rates of deletion resulting from a single selection and the double selection was probably due to intermolecular recombinations within the 2-kb sequence, which were not followed by an intramolecular recombination.

The high rates of deletion between two identical sequences within a retroviral RNA molecule are mostly due to interamolecular recombinations. This observation is consistent with the fact that the newly synthesized minus-strand DNA primers preferably anneal on the intra-RNA molecule rather than on the inter-RNA molecule (7). This suggests that the two RNA molecules are not randomly intertwined in a virion. Alternatively, the reverse transcriptase, with partially synthesized minus-strand DNA, may slide along with the template RNA molecule until the minus-strand DNA anneals at a homologous sequence within the same RNA molecule. Once DNA synthesis is completed, the resulting DNA would contain a deletion between the two identical sequences.

ACKNOWLEDGMENTS

We thank William Bargmann, Robert Jacob, Ting Li, and Alan Simmons for helpful comments on the manuscript.

This research was supported by Public Health Service research grant CA70407.

REFERENCES

1. **Adam, M. A., N. Ramesh, A. D. Miller, and W. R. Osborne.** 1991. Internal initiation of translation in retroviral vectors carrying picornavirus 5′ nontranslated regions. J. Virol. **65:**4985–4990.
2. **Boris-Lawrie, K. A., and H. M. Temin.** 1993. Recent advances in retrovirus vector technology. Curr. Opin. Genet. Dev. **3:**102–109.
3. **Coffin, J. M., S. H. Hughes, and H. Varmus**. 1997. Retroviruses. Cold Spring Harbor Laboratory Press, Plainview, N.Y.
4. **Dornburg, R., and H. M. Temin.** 1988. Retroviral vector system for the study of cDNA gene formation. Mol. Cell. Biol. **8:**2328–2334.
5. **Dougherty, J. P., and H. M. Temin.** 1987. A promoterless retroviral vector indicates that there are sequences in U3 required for 3′ RNA processing. Proc. Natl. Acad. Sci. USA **84:**1197–1201.
6. **Hu, W. S., and H. M. Temin.** 1990. Genetic consequences of packaging two RNA genomes in one retroviral particle: pseudodiploidy and high rate of genetic recombination. Proc. Natl. Acad. Sci. USA **87:**1556–1560.
7. **Jones, J. S., R. W. Allan, and H. M. Temin.** 1994. One retroviral RNA is sufficient for synthesis of viral DNA. J. Virol. **68:**207–216.
8. **Klaver, B., and B. Berkhout.** 1994. Premature strand transfer by the HIV-1 reverse transcriptase during strong-stop DNA synthesis. Nucleic Acids Res. **22:**137–144.
9. **Li, T., and J. Zhang.** 2000. Determination of the frequency of retroviral recombination between two identical sequences within a provirus. J. Virol. **74:**7646–7650.
10. **Lobel, L. I., and S. P. Goff.** 1985. Reverse transcription of retroviral genomes: mutations in the terminal repeat sequences. J. Virol. **53:**447–455.
11. **Miller, A. D., and C. Buttimore.** 1986. Redesign of retrovirus packaging cell lines to avoid recombination leading to helper virus production. Mol. Cell. Biol. **6:**2895–2902.
12. **Miller, A. D., J. V. Garcia, N. von Suhr, C. M. Lynch, C. Wilson, and M. V. Eiden.** 1991. Construction and properties of retrovirus packaging cells based on gibbon ape leukemia virus. J. Virol. **65:**2220–2224.
13. **Miller, A. D., and G. J. Rosman.** 1989. Improved retroviral vectors for gene transfer and expression. BioTechniques **7:**980–982, 984–986, 989–990.
14. **Ramsey, C. A., and A. T. Panganiban.** 1993. Replication of the retroviral terminal repeat sequence during in vivo reverse transcription. J. Virol. **67:** 4114–4121.
15. **Sambrook, J., E. F. Fritsch, and T. Maniatis.** 1989. Molecular cloning: a laboratory manual, 2nd ed. Cold Spring Harbor Laboratory, Cold Spring Harbor, N.Y.
16. **Sapp, C. M., T. Li, and J. Zhang.** 1999. Systematic comparison of a color reporter gene and drug resistance genes for the determination of retroviral titers. J. Biomed. Sci. **6:**342–348.
17. **Skalka, A. M., and S. Goff.** 1993. Reverse transcriptase. Cold Spring Harbor Laboratory Press, Plainview, N.Y.
18. **Watanabe, S., and H. M. Temin.** 1983. Construction of a helper cell line for avian reticuloendotheliosis virus cloning vectors. Mol. Cell. Biol. **3:**2241–2249.
19. **Zhang, J., and C. M. Sapp.** 1999. Recombination between two identical sequences within the same retroviral RNA molecule. J. Virol. **73:**5912–5917.
20. **Zhang, J., L. Y. Tang, T. Li, Y. Ma, and C. M. Sapp.** 2000. Most retroviral recombinations occur during minus-strand DNA synthesis. J. Virol. **74:**2313–2322.
21. **Zhang, J., and H. M. Temin.** 1993. 3′ junctions of oncogene-virus sequences and the mechanisms for formation of highly oncogenic retroviruses. J. Virol. **67:**1747–1751.
22. **Zhang, J., and H. M. Temin.** 1993. Rate and mechanism of nonhomologous recombination during a single cycle of retroviral replication. Science **259:** 234–238.
23. **Zhang, J., and H. M. Temin.** 1994. Retrovirus recombination depends on the length of sequence identity and is not error prone. J. Virol. **68:**2409–2414.